

APPLIED RESEARCH

Parameters Optimization of UAV for Insulator Inspection on Power Transmission Line

LIN YIN¹, JING HU¹, WENBIN WANG¹, JIACHEN ZOU^{1,2}, LINXUAN HE², ZHOU XIONG¹, MINGJUN LIU¹, FAN LI¹, AND YOUPIING TU^{1,2}

¹State Grid in Jiangxi Province and Power Company Ltd., Jiangxi 330029, China

²Beijing Key Laboratory of High Voltage and EMC, North China Electric Power University, Beijing 10096, China

Corresponding author: Youping Tu (typ@ncepu.edu.cn)

This work was supported in part by the Research on UAV Intelligent Analysis Technology for Key Business Links of Transmission and Distribution Lines under Grant SGJXDKOOPWJSJS2100227.

ABSTRACT In recent years, Unmanned Aerial Vehicle (UAV) technology has been widely used in power transmission line inspection. UAV operating parameters determine the quality of the acquired insulator image, which directly affects the efficiency of transmission line inspection. Regarding the inspection of ceramic insulators, this work establishes a three-dimensional (3D) model of ceramic insulators, and simulates the changes in shooting distance, angle, and height of the UAV through three geometric transformations: rotation, translation, and scaling. The influence of those three UAV operating parameters (the shooting distance, angle, and height) on the integrity of the ceramic insulator steel cap is studied. In the infrared zero value detection of 110kV ceramic insulators, It is found that the best setting for obtaining the maximum steel cap area is: shooting distance of 3–7 meters, shooting height of 1 meter below the center of the insulator string, and a shooting depression angle of 0°. The UAV operating parameters setting method proposed in this paper will provide theoretical and practical basis for the in-depth intelligent inspection of transmission line insulators.

INDEX TERMS UAV operating parameters, insulator, zero value defect, infrared detection.

I. INTRODUCTION

With the rapid development of the power industry and the grow of the power, traditional manual inspection methods can no longer meet the needs of modern power grid. UAV inspection is safe and efficient [1], [2]. Taking visible and infrared images of insulators and using image processing technology to detect defects has become the development direction of UAV power grid inspections. However, the integrity of the insulators in the image (insulators blocked, overlapping, and deformed) insufficient will cause problems such as low robustness on defect detection [3]–[5], resulting in poor detection results.

Several researchers have studied insulator identification and defect detection based on insulator images. Jiang *et al.* [6] proposed a method to identify insulators by combining the

color, shape and texture characteristics of insulators, and proposed a method to detect the defects of glass insulators based on the distance between the insulator plates. However, if the shooting distance is far, the influence of the background texture will increase, resulting in a decrease in the detection accuracy. Zhang *et al.* [7] identified insulator defects based on particle swarm optimization feedforward neural network He *et al.* [3] used the Faster R-CNN algorithm [8] to build an insulator detection model and locate the insulator target. Then, he realized the lack of defect discrimination of glass insulators through CNN algorithm. But when the adjacent insulators are blocked, the detection result was poor. Zhou [9] and others proposed a degraded insulator identification method based on the combination of time series model and infrared detection technology, but the steel cap area need to be separated from the infrared image. When the insulator steel cap is blocked by the adjacent insulator, it will decrease the detection accuracy. Therefore, by optimizing the operating parameters of the UAV and standardizing the

The associate editor coordinating the review of this manuscript and approving it for publication was Zheng H. Zhu ^{1,2}.

operating process of the UAV, the accuracy of the insulator defect detection can be effectively improved.

Regarding the optimization of UAV operating parameters, Yang from Jiangsu University [10] studied the best shooting point of UAV for the insulator inspection. The shooting method was preliminary studied by changing the shooting angle under a fixed shooting distance and height. Li *et al.* [11] qualitatively studied the influence of environmental humidity, occlusion, image clarity, and shooting distance on the infrared test results, but did not quantitatively explain the relationship. Considering there is limited research about the influence of the three parameters (shooting height, distance, and angle) on the completeness of insulator images, there is a lack of unified principles or methods for the selection of UAV operating parameters.

This paper established a 3D model of the ceramic insulator in CAD, and simulated the height, distance and angle of the insulator taken by the UAV through three geometric transformations: rotation, translation, and scaling. UAV operation parameter setting method was studied by judging the integrity of the target in the image. Ceramic insulators were used as examples to study the influence of operation parameters on steel cap integrity. The operation parameters of UAV inspection zero-value insulators that meet the requirements of image integrity evaluation were also proposed.

II. UAV OPERATING PARAMETERS AND GEOMETRIC TRANSFORMATION OF INSULATORS

An isometric model of the pendant insulator is established in CAD. Since the observation point of the insulator in CAD is fixed, specific operations such as rotating, zooming, and translating are performed on the insulator model to simulate the changes of UAV operating parameters in reality. The following analyzes the corresponding relationship between the zoom, translation, and rotation operations of the insulator and the changes in the height, angle, and distance of the drone. The equivalent correspondence between the changes of UAV operating parameters and the geometric transformation of insulators is shown in Figure 1.

Figure 1(a) shows the correspondence between the shooting height and the vertical shift of the insulator. The shooting height is linearly related to the vertical shift distance of the insulator, i.e., the increase of the shooting height x is equivalent to the downward shift of the insulator x .

Figure 1(b) shows the correspondence between the shooting distance and the scaling of the insulator. The longer the shooting distance, the smaller the proportion of the insulator in the screen. The shooting distance can be changed by scaling the insulator. The relationship between the shooting distance and the zoom ratio r_1 is shown in equation (1).

$$r_1 = \frac{a}{2d \tan \frac{\theta}{2}} \quad (1)$$

where θ is the UAV's field of view angle, a is the length of the insulator string, and d is the shooting distance.

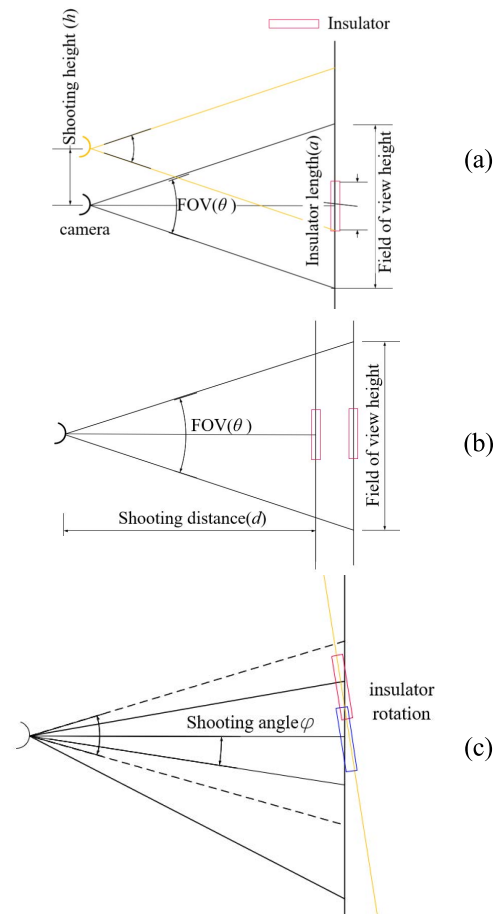


FIGURE 1. Correspondence diagram of insulator geometric transformation and operating parameters: (a) Shooting height and insulator displacement; (b) Shooting distance and insulator zoom; (c) Shooting angle and insulator zoom and rotation.

Figure 1(c) shows the corresponding relationship between the shooting angle and the scaling and rotation of the insulator. The shooting depression angle can be equivalent to rotating and scaling the insulator. The rotation method is by rotating the insulator string in the vertical direction with the UAV as the base point, and the rotation angle is equal to the shooting depression angle; the functional relationship between the shooting depression angle and the zoom ratio r_2 is shown in equation (2).

$$r_2 = \frac{2 \tan \frac{\theta}{2}}{\tan(\varphi + \frac{\theta}{2}) - \tan(\varphi - \frac{\theta}{2})} \quad (2)$$

By analyzing the corresponding relationship between the shooting height, distance, depression angle and the geometric transformation of the insulator, according to the superposition principle, the height, distance and angle of the insulator shooting by the UAV can be simulated.

III. INSULATOR IDENTIFICATION METHOD BASED ON IMAGE PROCESSING

The insulator used in this article is the XP-160 disc type suspension ceramic insulator. The cross-sectional view is

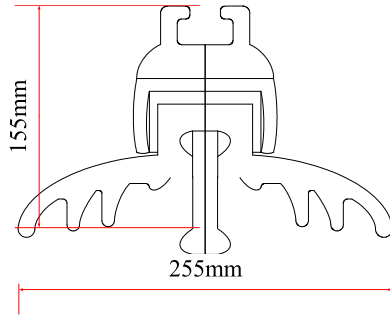


FIGURE 2. Sectional view of XP-160 insulator.

shown in Figure 2. The height is 155 mm and the nominal diameter is 255 mm.

A 110kV ceramic insulator string model was established in CAD, including 7 XP-160 ceramic insulators discs, with a length of 1.075 m. Its axonometric view is shown in Figure 3. The insulator image is obtained when the shooting distance is 5m, the shooting angle is 0° , and the shooting height is at the center of the insulator, as shown in Figure 4(a).

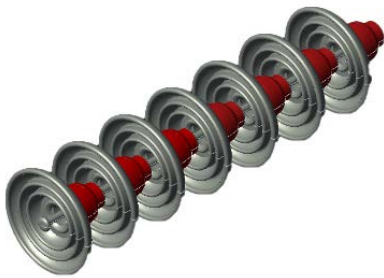


FIGURE 3. 110kV suspended insulator model axonometric drawing.

The insulators are segmented from the image using the threshold segmentation method based on RGB color components [12]–[14]. The RGB (Red, Blue, Green) components were extracted, the saturation of the insulator body and steel cap region in each component diagram were analyzed, and the optimal entropic threshold method (OET) [15] was used to separate the insulator body and steel cap. OET applies the concept of entropy to image segmentation to maximize the amount of information distributed between the target and the background in the image. The method also finds the optimal threshold by analyzing the entropy of the image gray histogram. For the disk surface, its contour characteristics are obvious, and the morphological method is used for disk surface segmentation [16]–[18].

The insulator body, steel cap, and disk surface were segmented using the above method. The segmentation result of the insulator body based on the G component are shown in Figure 4(b); the segmentation result of the steel cap region based on the R component is shown in Figure 4(c); and the disk area segmentation result based on contour features is shown in Figure 4(d).

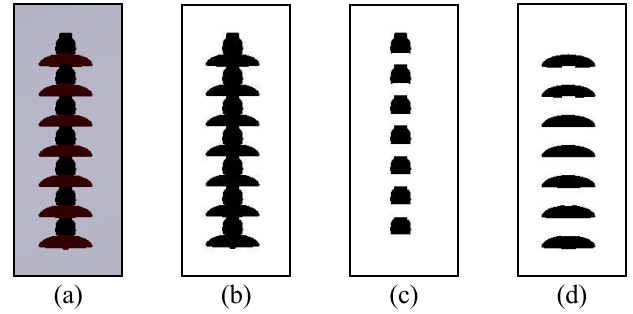


FIGURE 4. Insulator segmentation results: (a) Original picture of in-insulator; (b) Segmentation result of insulator string; (c) Segmentation result of the steel cap; (d) Segmentation result of the disk surface.

IV. CALCULATION METHOD OF OPERATING PARAMETERS FOR UAV INSULATOR INSPECTION

A. EVALUATION INDEX OF UAV SHOOTING RESULT

Insufficient image completeness of the insulator will cause the lack of key information in the image, which is one of the reasons for missed detection. The insulator area ratio is defined as the ratio of the insulator area to the reference area value. The insulator area ratio is used to quantify the integrity of the insulator image, where the area reference value is the total area of the insulator under unobstructed conditions. The closer this insulator area ratio is to 1, the more complete the insulator area in the image, the less overlap and occlusion.

For different types of insulator defects, the characteristic areas of concern are different, and appropriate evaluation indicators need to be determined according to the type of defect. The early decay of composite insulators is often manifested as abnormal heating of the sheath [18]–[22], and the integrity of the sheath can be used to quantitatively evaluate the infrared inspection image of the composite insulator. The zero-value insulator is mainly manifested as abnormal heating in the steel cap area [14], [23], and the inspection image of the zero-value insulator is based on the integrity of the steel cap. Taking zero-value insulator detection as an example, the calculation method of steel cap area ratio is as follows.

1) Obtain the insulator image when the depression angle is 0° and the UAV is flush with the low-voltage end; use the method in Section 2 to calculate the area of the first steel cap of the low-voltage end, and multiply it by the number of steel caps as the baseline of the steel cap area of the insulator S_e ;

2) Calculate the insulator image acquired at the set shooting depression angle and height, and use the method in Section 2 to calculate the area S of the insulator's steel cap;

3) Calculate the area ratio of steel cap S/S_e

B. UAV OPERATION PARAMETER TUNING CALCULATION PROCESS

Many factors need to be considered in the setting calculation of the operating parameters of the insulator of the UAV inspection line. For example, the shooting distance cannot be

less than the safety distance (related to the line voltage level); in order to ensure the cleanness of the image, the shooting distance cannot be too far; the selected three operating parameters need to make the UAV capture full insulator strings and etc. By analyzing these factors, the operating parameter range was set, so as to formulate the setting calculation process as shown in Figure 5. The formulation of the setting calculation process is illustrated by taking the UAV inspection of 110kV zero-value insulators as an example.

Considering the safety distance, image clarity, and the degree of overlap and deformation of insulators [9], the shooting distance and shooting depression angle are considered as constraint variables, and the range of variation is determined accordingly. The shooting distance is 3m~10m, and the shooting depression angle is $-30^{\circ}\sim 30^{\circ}$. At the same time, in order to obtain the image of the entire insulator, the operating parameters of the UAV are constrained. Since changing the shooting height only needs to translate the insulator, which is a simple operation, and the size of the insulator is not changed, so the shooting height is constrained, and the constraint equation is shown in equation (3).

$$d \tan(\varphi - \frac{\theta}{2}) + \frac{a}{2} < h < d \tan(\varphi + \frac{\theta}{2}) - \frac{a}{2} \quad (3)$$

A 3D model of 110kV insulator is built in CAD, and the calculation process of operating parameter setting is shown below. In this paper, the height of the center of the insulator is 0m, and the direction of the low-voltage end is the positive direction.

- 1) Initialization of UAV operating parameters, shooting depression angle, shooting distance, shooting height;
- 2) Determine whether the shooting depression angle is within $-30^{\circ}\sim 30^{\circ}$, if so, traverse the shooting height starting from the lowest allowable height, increasing by 0.1 m each time, otherwise initialize the operating parameters;
- 3) Determine whether the shooting height satisfies the equation (3), if so, execute the JPGOUT command in the CAD to output the insulator image. Otherwise, the shooting depression angle will increase by 5° , and return to step 2);
- 4) Calculate the steel cap area ratio of the image, and output the three UAV operating parameters when the insulator area ratio is the largest.

After the operation parameters are initialized for the second time, change the shooting distance and height, and repeat steps 1) to 4).

V. OPERATIONAL PARAMETER TUNING RESULTS OF UAV INSPECTION FOR ZERO VALUE OF CERAMIC INSULATORS

A. THE INFLUENCE OF OPERATING PARAMETERS ON THE INTEGRITY OF STEEL CAPS

In this section, typical shooting positions to obtain insulator images within the setting range were selected, the area ratio of steel caps was calculated respectively. The influence of operating parameters on the integrity of steel caps was explored,

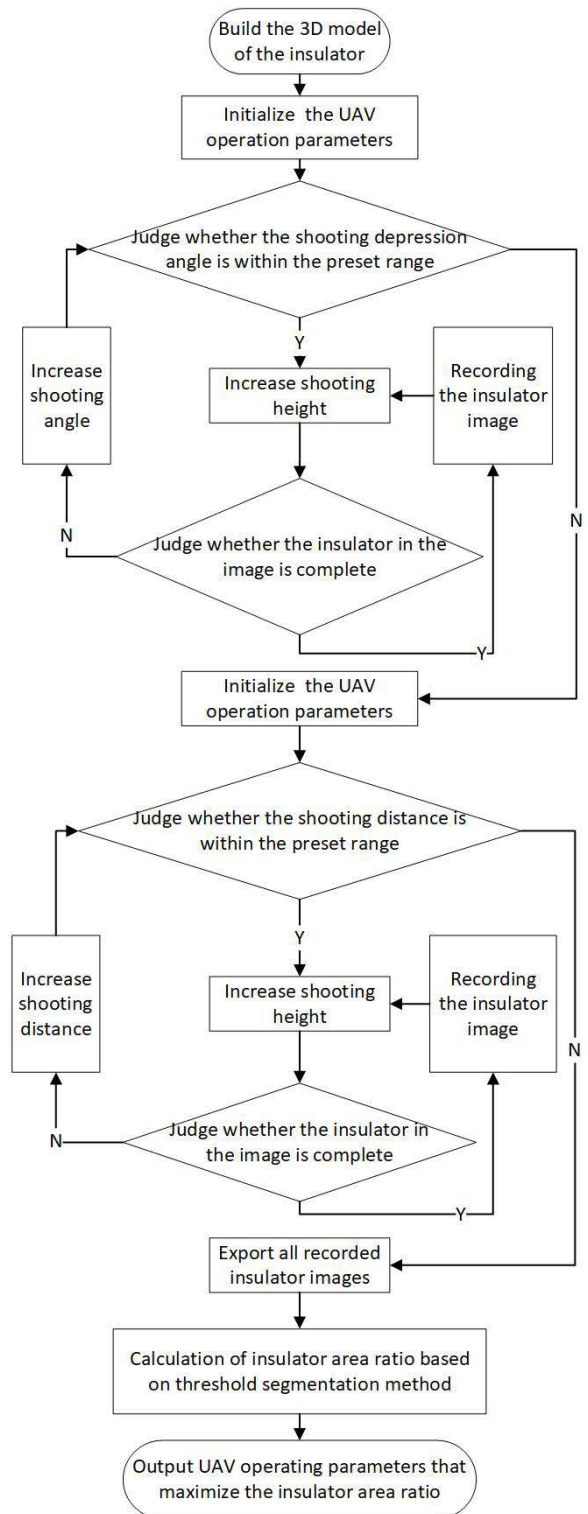


FIGURE 5. The UAV operation parameter setting calculation process.

and an optimal plan for operating parameters selection was proposed.

The variation law of steel cap area ratio with shooting depression angle and shooting height is shown in Figures 6 and 7. The x axis is the shooting height, and the

y axis is the steel cap area ratio. When the depression angle is greater than or equal to 0°, the area ratio of the steel cap gradually decreases with the increase of the height, and when the depression angle is less than or equal to -10°, the area ratio of the steel cap gradually increases with the increase of the height, where the area ratio of the steel cap is -5°. The relationship with height is parabolic, and -5° is considered to be a threshold angle for this regular transformation.

As the shooting height increases, the position of the insulator string in the image moves down relatively, and the top of the steel cap is blocked by the disk of the upper insulator, resulting in a decrease in the integrity of the steel cap. When this shielding effect is strengthened, it will result in a further reduction in the integrity of the steel cap. When the UAV is shooting from a low angle, the bottom area of the steel cap will be blocked by its own insulator plate, resulting in a decrease in the integrity of the steel cap. Therefore, there must be a threshold angle between the shooting depression angles of different blocking directions, determined by the structure and shape of the insulator.

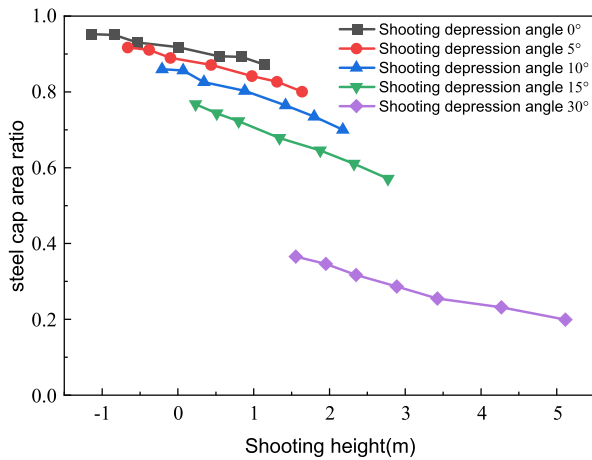


FIGURE 6. The curve of steel cap area ratio with shooting height and depression angle.

The change of steel cap area ratio with shooting distance and shooting height is shown in Figure 8. Within the shooting distance of 3 m~10 m, the steel cap area ratio changes with the shooting height. The closer the shooting distance, the more occlusion of the steel cap, resulting in a reduction in the maximum value of the steel cap area ratio. When the shooting distance is 7m, the maximum steel cap area ratio reaches the maximum. But when the shooting distance is between 3m and 7m, the difference in the area ratio of the steel cap is within 0.02. When the shooting distance continues to increase, the image clarity becomes the main factor affecting the area ratio of the steel cap, resulting in rapidly decrease of the steel cap area. Therefore, the best shooting distance is 3 m~7 m.

B. THE RESULT OF OPERATING PARAMETER TUNING

According to the above analysis, on the premise of obtaining the image of the entire insulator, in order to maximize the area

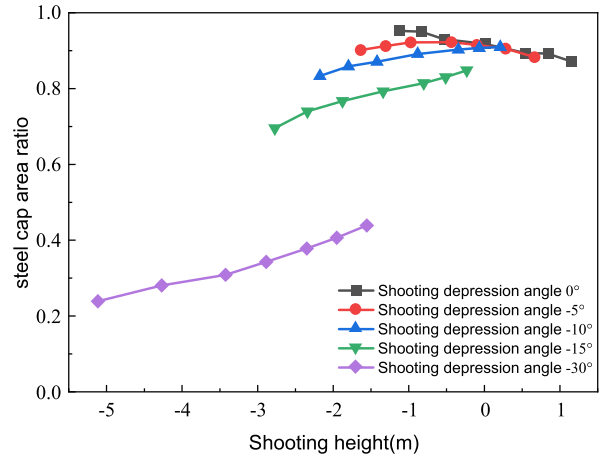


FIGURE 7. The trend of steel cap area ratio with shooting height and depression angle.

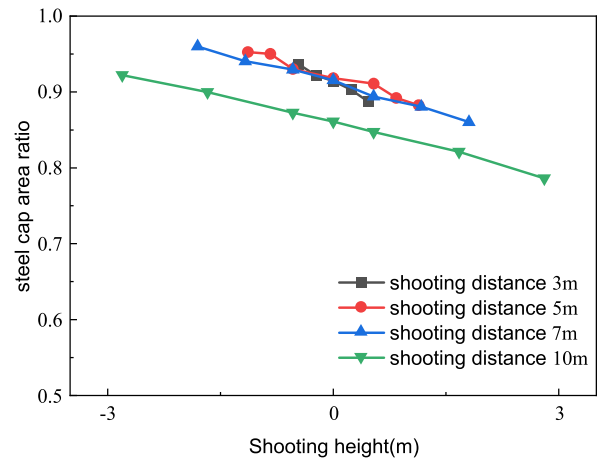


FIGURE 8. The change curve of steel cap area ratio with shooting height and distance.

ratio of the insulator steel cap, the shooting distance should be 3-7m. The constraint condition of the shooting distance d is expressed in equation (4). The structure and shape of the insulator determine the value of the threshold angle. When the shooting depression angle is greater than the threshold angle, the shooting height should be taken as the lowest height for obtaining the entire insulator image, as shown in equation (5). When the shooting depression angle is less than the threshold angle, the shooting height should be the highest height to capture the entire insulator, as expressed in equation (6).

$$d > \frac{a}{2 \tan \frac{\theta}{2}} \text{ 且 } 3 < d < 7 \tag{4}$$

$$h_f = d \tan(\varphi - \frac{\theta}{2}) + \frac{a}{2} \tag{5}$$

$$h_y = d \tan(\varphi + \frac{\theta}{2}) - \frac{a}{2} \tag{6}$$

This paper has discussed the optimization of inspection parameters for vertical pendant insulators. When facing a porcelain insulator in a horizontal or inclined state, the

reference coordinate system of the UAV operating parameters can be rotated so that the reference coordinate system and the insulator axis are always consistent. Coincidence, when the lens is perpendicular to the axis of the insulator, is regarded as the shooting angle of 0°, which is consistent with the discussion of the pendant insulator in the vertical direction.

VI. APPLICATION OF UAV INSPECTION ON THE ZERO VALUE OF CERAMIC INSULATOR

Sections 4 and 5 have presented the calculation method for parameter of UAV insulator inspection and the result of parameter setting of zero value insulator inspection. Here, the operating parameters of onsite UAV would be adjusted and calculated based on the above method to verify the simulation results obtained in Section 5.2.

Taking a 110kV line suspension insulator as the study object, M300-H20T was used to take infrared images of insulators. The field of view of the equipment is 25°, the shooting distance is 5m, and the insulator string length *a* is 1.075m. The shooting environment conditions are: the ambient temperature is 31°C, the ambient humidity is 60%, the ground wind speed is 0, and the light intensity is 2100 lx. A typical infrared image is shown in Figure 9

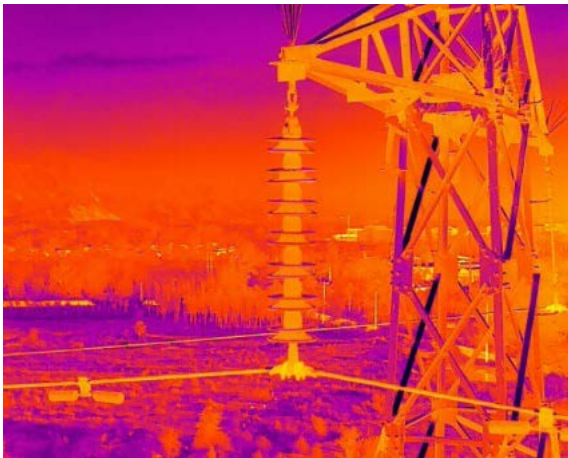


FIGURE 9. Infrared image of 110kV suspension insulator.

The steel cap area ratio of infrared images taken by M300-H20T at different shooting heights and depression angles are calculated, and the results are shown in Figure 10 and 11. The shooting height of 0m is the height of the center of the insulator, and the direction of the low-voltage side is the square phase. When the insulator is shot down, as the height increases, the area ratio of the steel cap gradually decreases, and as the depression angle increases, the area ratio of the steel cap decreases gradually, which is consistent with the simulation results obtained in Section 5.2. When shooting the insulator upside down, the area ratio of the steel cap decreases gradually with the increase of the elevation angle; the change rule of the area ratio of the steel cap with the shooting height is affected by the elevation angle. When the elevation angle is 5°, the relationship between the steel cap

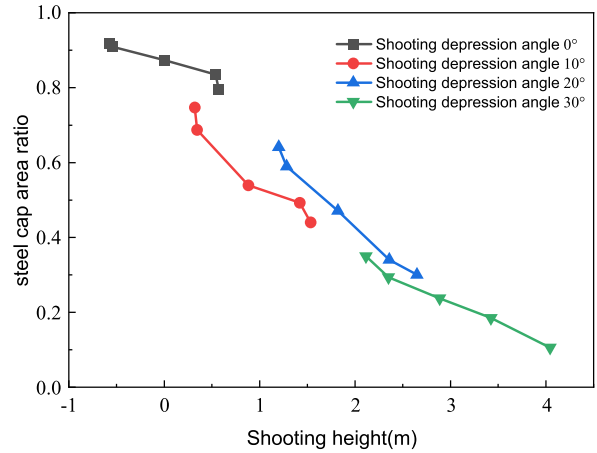


FIGURE 10. The variation curve of steel cap area ratio with height and depression angle under experimental conditions.

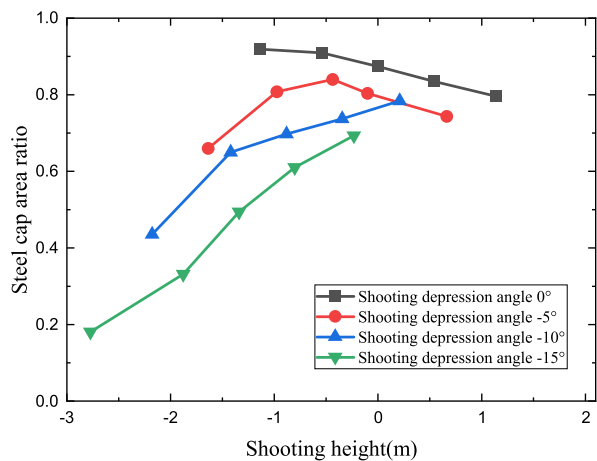


FIGURE 11. The variation curve of steel cap area ratio with height and depression angle under experimental conditions.

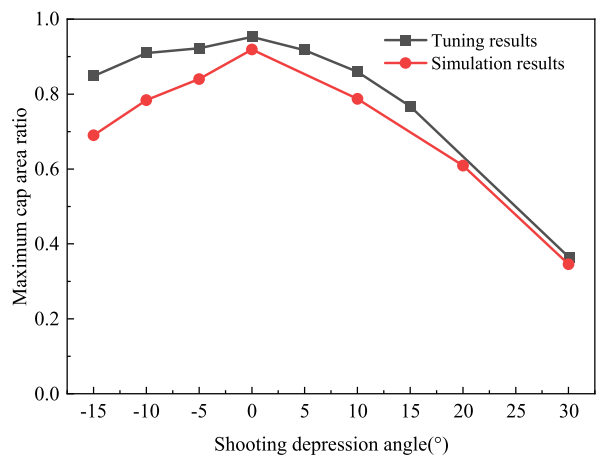


FIGURE 12. The relationship between depression angle and maximum steel cap area ratio under simulation and experimental conditions.

area ratio and the shooting height is parabolic, and it gradually transforms into a monotonically increasing curve after the elevation angle continues to increase, which is consistent with the simulation results obtained in Section 5.2.

According to the simulation results obtained in Section 5.2 and the field experiment results, the variation of the maximum steel cap area ratio with the shooting depression angle is compared, as shown in Figure 12. It can be found from the figure that the area ratio of the steel cap in the field experiment is slightly lower than the area ratio of the simulated steel cap, but the absolute error is within 0.14. The reason may be that the top end of the steel cap under the experimental conditions is affected by the shading of the upper disk surface, which results in the visual darkening, making it difficult to be identified as a steel cap.

VII. CONCLUSION

According to the purpose of inspection, the integrity of the target area is selected as the evaluation index of the UAV's shooting effect, and the operating parameter calculation process is formulated considering factors such as safety distance and image clarity. The operating parameter calculation method of the insulator for the UAV line inspection is proposed. The influence of the shooting height, distance and angle on the integrity of the steel cap is obtained by calculation, and the above influence is verified through field experiments. The optimal operation parameter scheme for obtaining the zero defect of the line insulator is proposed. Regarding the UAV inspection of 110kV line zero-value insulators, the main conclusions of this paper are as follows:

1) When the shooting distance remains the same and the shooting depression angle is within $[0^\circ, 30^\circ]$, the obtained steel cap area ratio will decrease as the shooting height increases; when the shooting depression angle is -5° , the obtained steel cap area ratio will first increase and then decrease as the shooting height increases. When the shooting depression angle is $[-1^\circ, -30^\circ]$, the obtained steel cap area ratio will increase as the shooting height increases.

2) When the shooting depression angle remains the same, as the shooting distance increases, the maximum value of the steel cap area ratio first increases and then decreases. When the shooting distance is 7 m, the maximum value of the steel cap area ratio reaches the maximum. However, the shooting distance is within 3 m – 7 m, the difference between the area ratio of the steel cap is within 0.02. When the shooting distance continues to increase, the image clarity decreases, resulting in a rapid decrease in the maximum value of the steel cap area ratio.

3) The shooting distance should be within 3 m~7 m. When the shooting angle is not less than 0° , the shooting height should be the lowest height that can capture the entire insulator. If the shooting angle is not greater than -10° , the shooting height should be the highest height that can capture the entire insulator.

REFERENCES

- [1] G. Xiaodong, T. Danhong, and H. Xiaohua, "Deep learning-based defect detection and recognition of a power grid inspection image," *Power Syst. Protection Control*, vol. 49, no. 5, pp. 91–97, 2021.
- [2] L. Xin, H. Jin, Y. Tu, Z. Yuan, Z. Lv, and C. Wang, "Defect detection and characterization of RTV silicone rubber coating on insulator based on visible spectrum image," *IEEE Trans. Power Del.*, vol. 35, no. 6, pp. 2734–2736, Dec. 2020.
- [3] N. H. He and S. J. Wang, "Research on infrared image missing insulator detection method based on deep learning," *Power Syst. Protection Control*, vol. 49, no. 12, pp. 132–140, 2021.
- [4] X. Jianjun, H. Lida, Y. Limei, and Y. Na, "Insulator self-explosion defect detection based on hierarchical multi-task deep learning," *Trans. China Electrotechnical Soc.*, vol. 36, no. 7, pp. 1407–1415, 2021.
- [5] Y. Liu, H. B. Chen, and F. Liu, "Research and application of intelligent perception system for unmanned aerial vehicle inspection at construction site," *Power Syst. Protection Control*, vol. 50, no. 5, pp. 52–58 and 64, 2017.
- [6] Y. T. Jiang, J. Han, J. Ding, H. N. Fu, Y. F. Wang, and W. Cao, "The identification and diagnosis of self-blast defects of glass insulators based on multi-feature Fu," *Electr. Power*, vol. 46, no. 15, pp. 155–161, 2018.
- [7] D. D. Zhang, "Detection of self-explosion position of insulator based on aerial image," M.S. thesis, Control Eng., XiHua Univ., Chengdu, China, 2018.
- [8] C. Cao, B. Wang, W. Zhang, X. Zeng, X. Yan, Z. Feng, Y. Liu, and Z. Wu, "An improved faster R-CNN for small object detection," *IEEE Access*, vol. 7, pp. 106838–106846, 2019, doi: [10.1109/ACCESS.2019.2932731](https://doi.org/10.1109/ACCESS.2019.2932731).
- [9] Y. Zhou, J. Yao, X. Wang, K. Li, Z. Liu, Y. Lu, and J. Yin, "Infrared image detection for faulty insulators based on time series model," *Insulators Surge Arresters*, vol. 1, 2020, Art. no. 149155, doi: [10.16188/j.isa.1003-8337.2020.01.025](https://doi.org/10.16188/j.isa.1003-8337.2020.01.025).
- [10] D. Liu, "Research on remote intelligent image recognition inspection technology for transmission lines," M.S. dissertation, Jiangsu Univ., Zhenjiang, China, 2019.
- [11] T. Li, L. Liu, Y. F. Chao, S. H. Wang, and L. Y. Zhou, "Research status of overhead line composite insulator field infrared test," *Water Resour. Power*, vol. 38, no. 8, pp. 184–187, 2020.
- [12] Z. B. Qiu, X. B. Yu, F. Huo, Z. Liu, W. X. Gong, and X. X. Zhou, "Spray image processing of composite insulators based on interval classification of uniformity measu," *High Voltage Eng.*, vol. 46, no. 9, pp. 3008–3017, 2020.
- [13] X. Chen and H. Chen, "A novel color edge detection algorithm in RGB color space," in *Proc. IEEE 10th Int. Conf. Signal Process.*, Oct. 2010, pp. 793–796, doi: [10.1109/ICOSP.2010.5655926](https://doi.org/10.1109/ICOSP.2010.5655926).
- [14] Y. Zhang, J. Tian, M. Yang, Y. Yi, Y. Wang, and Y. Zhang, "Screening of zero-value insulators infrared thermal image features based on binary logistic regression analysis," in *Proc. 2nd IEEE Conf. Energy Internet Energy Syst. Integr. (EI)*, Oct. 2018, pp. 1–4, doi: [10.1109/EI2.2018.8582434](https://doi.org/10.1109/EI2.2018.8582434).
- [15] L. Wang, "Research on threshold segmentation algorithm based on OTSU and maximum entropy," M.S. dissertation, Harbin Univ. Sci. Technol., Harbin, China, 2018.
- [16] G. J. Xu, "Image edge detection algorithms based on morphological gradients," M.S. dissertation, Xidian Univ., Xi'an, China, 2013.
- [17] Z. Yuan, Y. Tu, Y. Zhao, H. Jiang, and C. Wang, "Analysis on heat source of abnormal temperature rise of composite insulator housings," *IEEE Trans. Dielectr. Electr. Insul.*, vol. 24, no. 6, pp. 3578–3585, Dec. 2017.
- [18] J. Yin, Y. Lu, Z. Gong, Y. Jiang, and J. Yao, "Edge detection of high-voltage porcelain insulators in infrared image using dual parity morphological gradients," *IEEE Access*, vol. 7, pp. 32728–32734, 2019, doi: [10.1109/ACCESS.2019.2900658](https://doi.org/10.1109/ACCESS.2019.2900658).
- [19] Z. Yuan, Y. Tu, R. Li, F. Zhang, B. Gong, and C. Wang, "Review on the characteristics, heating sources and evolutionary processes of the operating composite insulators with abnormal temperature rise," *CSEE J. Power Energy Syst.*, vol. 8, no. 3, pp. 910–921, May 2022, doi: [10.17775/CSEEJPES.2019.02790](https://doi.org/10.17775/CSEEJPES.2019.02790).
- [20] H. Jin, Z. Lv, Z. Yuan, Z. Wei, C. Wang, C. Wang, Y. Tu, F. Li, T. Chen, and P. Xiao, "Micro-cracks identification and characterization on the sheds of composite insulators by fractal dimension," *IEEE Trans. Smart Grid*, vol. 12, no. 2, pp. 1821–1824, Mar. 2021.
- [21] C. Z. Xie, L. L. Zeng, Y. Y. Gan, C. Ben, and F. S. Zhou, "Study on pyrolysis characteristics of fiber reinforced plastic rod of composite insulators based on TG-FTIR analysis," *Trans. China Electrotechnical Soc.*, vol. 33, no. S1, pp. 227–233, 2018.

- [22] L. Te, Z. Luyao, D. Yu, L. Minglei, W. Shao-Hua, and W. Dian, "Comparative research of laboratory and field infrared test of 500 kV transmission line composite insulator," in *Proc. IEEE Int. Conf. High Voltage Eng. Appl. (ICHVE)*, Sep. 2020, pp. 1–4, doi: 10.1109/ICHVE49031.2020.9280020.
- [23] Y. Cheng, L. Z. Xia, Z. F. Li, D. F. Cheng, B. Yan, and S. S. Li, "Detection of faulty porcelain insulator based on infrared imaging method," *Insul. Mater.*, vol. 52, no. 3, pp. 74–79, 2019.



LIN YIN was born in 1984. He received the bachelor's degree. He is a Senior Engineer with the Transmission Department of the Equipment Department of State Grid Jiangxi Electric Power Company Ltd. He is the Outstanding Young Post Expert in Jiangxi and a member of the 10th Committee of Jiangxi Youth Federation. He has long-term experience in power transmission lines (high-voltage cables) design, planning, construction, operation, maintenance, and maintenance management. He has presided over the research project of a full-time automatic welding robot for the comprehensive construction platform of transmission lines and substation grounding relying on new engineering technology and presided over the research of major scientific and technological projects on the prevention and application of geological disasters on the transmission lines of Jiangxi Power Grid.



JING HU received the Ph.D. degree. He is a Senior Engineer and the Director of the Electric Power Research Institute of State Grid Jiangxi Electric Power Company Ltd., where he has long been engaged in technical management of transmission line operation and maintenance and related scientific research.



WENBIN WANG is pursuing the master's degree. His research interest includes artificial intelligence technology for power grid equipment.



JIACHEN ZOU was born in Ganzhou, Jiangxi, China, in 1997. He received the B.Sc. degree in electrical engineering from North China Electric Power University, Beijing, in 2020. His research interest includes outdoor insulation.



LINXUAN HE was born in Xingtai, Hebei, China, in 1997. He received the B.Sc. degree in control technology and instruments from North China Electric Power University, Beijing, in 2019. His research interest includes outdoor insulation.

ZHOU XIONG, photograph and biography not available at the time of publication.



MINGJUN LIU received the Ph.D. degree. He is a Senior Engineer. His main research interests include research and application of on-line monitoring of substation equipment status and live detection technology.



FAN LI was born in 1989. He received the B.Sc. degree in control technology and instruments from North China Electric Power University, Beijing, in 2015. He is the Director of the Electric Power Research Institute of State Grid Jiangxi Electric Power Company Ltd., the Secretary-General of the IEEE PES Substation Technical Committee (China), the Deputy Secretary-General of the IEEE PES Intelligent Inspection Subcommittee (China), and the Power Industry Transmission and Distribution Technology Cooperation Network (EPTC) Expert Member of the UAV Technology Working Group, a member of the Jiangxi State-Owned Enterprise Youth Federation, and the Vice Chairperson of the Executive Committee. His research interests include artificial intelligence, state evaluation of power transmission, and transformation equipment.



YOUPIING TU was born in July 1966. She received the bachelor's and master's degrees from Chongqing University, in 1988 and 1991, respectively. She is currently a Professor and the Ph.D. Supervisor with the School of Electrical and Electronic Engineering of North China Electric Power University. Her main scientific research projects are responsible for four National Natural Science Foundation projects, one National 973 Program project, one National Key Research and Development Program sub-project, one National Science and Technology Support Program sub-project, and participates in the national major plan special project as a Core Member of the project team International Thermonuclear Experimental Reactor (ITER) project, presided over nearly 15 horizontal projects. Published one textbook, published more than 200 papers included in SCI and EI. She received two provincial and ministerial second prizes, four third prizes, and 15 invention patents.

...